



Article

Kingsgateite, $\text{ZrMo}_2^{6+}\text{O}_7(\text{OH})_2 \cdot 2\text{H}_2\text{O}$, the first natural zirconium molybdate from Kingsgate, New South Wales, Australia

Peter Elliott^{1,2*}  and Anthony R. Kampf³ 

¹Department of Earth Sciences, School of Physical Sciences, The University of Adelaide, Adelaide, South Australia 5005, Australia; ²South Australian Museum, North Terrace, Adelaide, South Australia 5000, Australia and ³Mineral Sciences Department, Natural History Museum of Los Angeles County, 900 Exposition Boulevard, Los Angeles, CA 90007, USA

Abstract

Kingsgateite, $\text{ZrMo}_2^{6+}\text{O}_7(\text{OH})_2 \cdot 2\text{H}_2\text{O}$, is a new supergene mineral from the Old 25 Pipe, Kingsgate, Gough Co., New South Wales, Australia. The mineral occurs in cavities in a quartz, muscovite matrix associated with molybdenite, gelosaitite and mambertiite. It forms yellowish green to bluish grey, square tabular crystals to 0.12 mm across. Kingsgateite has a white streak and a vitreous lustre. Cleavage was not observed and the fracture is uneven. The calculated density is 3.74 g/cm^{-3} based on the empirical formula. Kingsgateite is optically biaxial (+), the calculated indices of refraction are $\alpha = 1.88$, $\beta = 1.89$, $\gamma = 1.96$ and $2V_{\text{calc}} = 42.6^\circ$. The pleochroism is $X = \text{light orange}$, $Y = \text{light yellow}$ and $Z = \text{red brown}$; $Y < X < Z$. The mineral is tetragonal, space group $I4_1cd$, $a = 11.4626(16)$, $c = 12.584(3) \text{ \AA}$, $V = 1653.4(6) \text{ \AA}^3$ and $Z = 8$. Electron microprobe analysis yielded ZrO_2 23.09, UO_2 1.14, ThO_2 0.76, FeO 0.62, MoO_3 59.27, P_2O_5 0.29, SO_3 1.25, Cl 0.16, H_2O 11.62, $\text{O}=\text{Cl} -0.04$, total 98.16 wt.%. The empirical formula on the basis of 11 anions per formula unit is $\text{Zr}_{0.88}\text{U}_{0.02}\text{Th}_{0.01}\text{Fe}_{0.04}\text{Mo}_{1.94}\text{S}_{0.07}\text{P}_{0.02}\text{O}_{6.90}\text{Cl}_{0.02}\text{OH}_{2.08} \cdot 2.00\text{H}_2\text{O}$. The crystal structure of kingsgateite, refined using synchrotron single-crystal data [$R_1 = 4.53\%$ for 1159 reflections with $F_o > 4\sigma(F_o)$], is a framework of edge- and corner-sharing $\text{ZrO}_5(\text{OH})_2$ pentagonal bipyramids and $\text{MoO}_4(\text{OH})(\text{H}_2\text{O})$ octahedra. Kingsgateite is isostructural with the synthetic compound $\text{ZrMo}_2^{6+}\text{O}_7(\text{OH})_2 \cdot 2\text{H}_2\text{O}$.

Keywords: kingsgateite, new mineral species, zirconium molybdate, crystal structure, Kingsgate, Australia

(Received 22 February 2022; accepted 19 April 2022; Accepted Manuscript published online: 27 April 2022; Associate Editor: Peter Leverett)

Introduction

Kingsgateite is the first natural zirconium molybdate. It is the natural analogue of the synthetic compound $\text{ZrMo}_2\text{O}_7(\text{OH})_2(\text{H}_2\text{O})_2$ (ICSD #9469) that has been prepared by refluxing zirconium molybdate gels in a strong hydrochloric acid solution (Clearfield and Blessing, 1972). Specimens of kingsgateite were collected from the dumps of the Old 25 Pipe, Kingsgate, Gough Co., New South Wales, Australia in 2015. The new mineral is part of a suite of secondary bismuth, molybdate, tungstate, phosphate and arsenate minerals. Thirty six valid mineral species with essential zirconium were known until now. More than half of these are oxides or silicates. Kingsgateite is the fourteenth zirconium mineral that is not an oxide or silicate. Kingsgateite is named for its type locality. The new mineral and its name (symbol Kgg) have been approved by the Commission on New Minerals, Nomenclature and Classification of the International Mineralogical Association (IMA 2019-048, Elliott and Kampf, 2019). The holotype specimen is deposited in the mineralogical collections of the South Australian Museum, Adelaide, South Australia, Registration number G34799.

Occurrence

The Kingsgate mines are situated in rugged, heavily wooded country at the eastern edge of the highly mineralised New England Tableland and comprise more than 60 workings, shafts, tunnels and small open cuts (England, 1985). The deposit was first exploited for tin in the late 1800s, but grades were too low to be profitable. The discovery of native bismuth, bismuthinite and molybdenite resulted in intermittent mining until the 1950s for bismuth, molybdenum and piezo-electric quartz. The deposit has produced outstanding specimens of bismuth, molybdenite and quartz. Mineralisation occurs in quartz pipes that are contained in a coarse, mottled grey hornblende–biotite granite. More than 70 pipes have been mapped and show an unusually complex structure. The Old 25 Pipe is one of the larger pipes and was worked by opencut and stoping to a depth of 250 feet. Records are incomplete, but at least 350 tonnes of molybdenite and 200 tonnes bismuth are known to have been produced. The major primary minerals are native bismuth, bismuthinite and molybdenite (Lawrence and Markham, 1962; Clissold *et al.*, 2008) with lesser amounts of other sulfides. A suite of secondary minerals, including molybdates, tungstates, phosphates and arsenates including such minerals as ferrimolybdate, gelosaitite, wulfenite, powellite, scorodite and carminite, have been described by England (1985) and Sharpe and Williams (2004). During the present study, mambertiite and tancaite-(Ce) have also been identified. Secondary minerals have formed under supergene conditions at low pH and low temperature.

*Author for correspondence: Peter Elliott, Email: peter.elliott@adelaide.edu.au

Cite this article: Elliott P. and Kampf A.R. (2022) Kingsgateite, $\text{ZrMo}_2^{6+}\text{O}_7(\text{OH})_2 \cdot 2\text{H}_2\text{O}$, the first natural zirconium molybdate from Kingsgate, New South Wales, Australia. *Mineralogical Magazine* 86, 486–491. <https://doi.org/10.1180/mgm.2022.43>

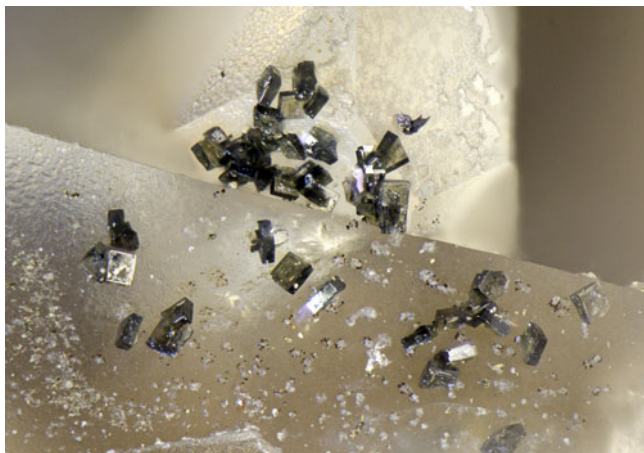


Fig. 1. Tabular crystals of kingsgateite on quartz. The field of view is 1 mm across.

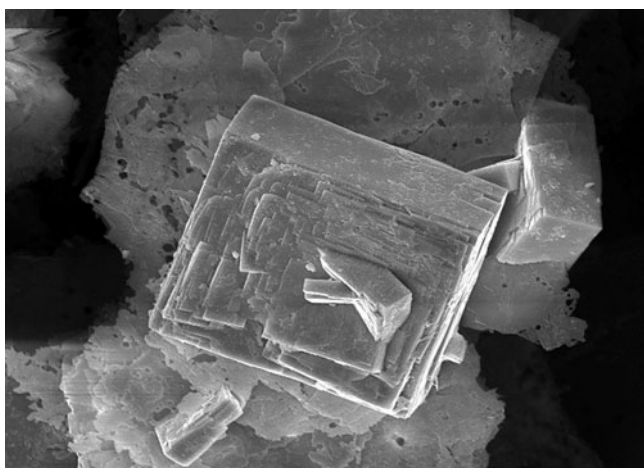


Fig. 2. Scanning electron microscopy photomicrograph showing a tabular crystal of kingsgateite 40 μm across on muscovite.

Kingsgateite occurs in cavities in a matrix comprised of quartz and minor muscovite. Associated minerals are molybdenite, gelsaite and mambertiite. Kingsgateite is the last mineral to be formed in the assemblage and is observed overgrowing molybdenite and gelsaite. Kingsgateite is the first mineral containing Zr to be recorded from Kingsgate. Accessory zircon in the host granite is probably the source of Zr, although it has not been recorded from the locality.

Physical and optical properties

Kingsgateite crystals are tabular in habit, with a maximum dimension of ~ 0.12 mm (Figs 1 and 2). Very small crystals are yellowish green in colour and transparent, larger crystals are bluish grey. Crystal forms are $\{001\}$ and probably $\{100\}$. The lustre is vitreous, and the streak is white. The mineral is brittle; the hardness could not be determined because of the small size of the crystals. The fracture is uneven and we did not observe signs of a distinct cleavage. Density was not measured because of the scarcity of available material; the calculated density based on the empirical formula is 3.74 g/cm^3 . Kingsgateite exhibits anomalous biaxial (+) optics manifest as sector growth (Fig. 3). The sector growth, small crystal size and high indices of refraction prevented the measurement of



Fig. 3. Kingsgateite crystal showing anomalous birefringence. The image is looking down the c axis under crossed polars with the crystal 45° from the extinction position and the gypsum (first-order red) plate inserted with its slow direction oriented NE–SW.

Table 1. Analytical data (wt.%) for kingsgateite.

Constituent	Wt.%	Range	S.D.	Probe standard
ZrO ₂	23.09	22.81–23.52	0.25	zircon
UO ₂	1.14	0.93–1.32	0.10	UO ₂
ThO ₂	0.76	0.58–0.95	0.10	huttonite
FeO	0.62	0.54–0.74	0.06	almandine
MoO ₃	59.27	58.07–60.09	0.57	molybdenum
P ₂ O ₅	0.29	0.26–0.32	0.02	apatite
SO ₃	1.25	1.21–1.32	0.03	chalcocopyrite
Cl	0.16	0.14–0.18	0.01	tugtupite
H ₂ O*	11.62			
O=Cl	–0.04			
Total	98.16			

* Calculated from the ideal formula.

S.D. – standard deviation

the indices of refraction. The Gladstone–Dale relationship predicts an average index of refraction of 1.905 for the ideal formula. The indices of refraction based on this average and on birefringence measurements: ($\gamma - \alpha = 0.08$ and $\beta - \alpha = 0.01$) are $\alpha = 1.88$, $\beta = 1.89$, $\gamma = 1.96$, providing $2V$ (calc.) = 42.6° . However, phases containing Mo⁶⁺ with short Mo=O bonds generally have higher average indices of refraction than those predicted by Gladstone–Dale, so the actual indices of refraction are likely to be significantly higher. Pleochroism is X and Y = colourless, Z = blue; $X = Y \ll Z$. Dispersion could not be observed.

Chemical composition

A small group of kingsgateite crystals was mounted in epoxy, polished, and carbon coated. Quantitative chemical analysis was obtained using a Cameca SXFive electron microprobe working in wavelength-dispersion mode with an accelerating voltage of 15 kV, beam current = 20 nA and beam diameter = 5 μm . Analytical data (12 analysis points) are given in Table 1. No other elements were detected by energy dispersive spectroscopy. The raw data were reduced with the PAP routine of Pouchou and Pichoir (1985). Because insufficient material is available for a direct determination of H₂O, it has been calculated based upon the structure determination. The presence of H₂O was

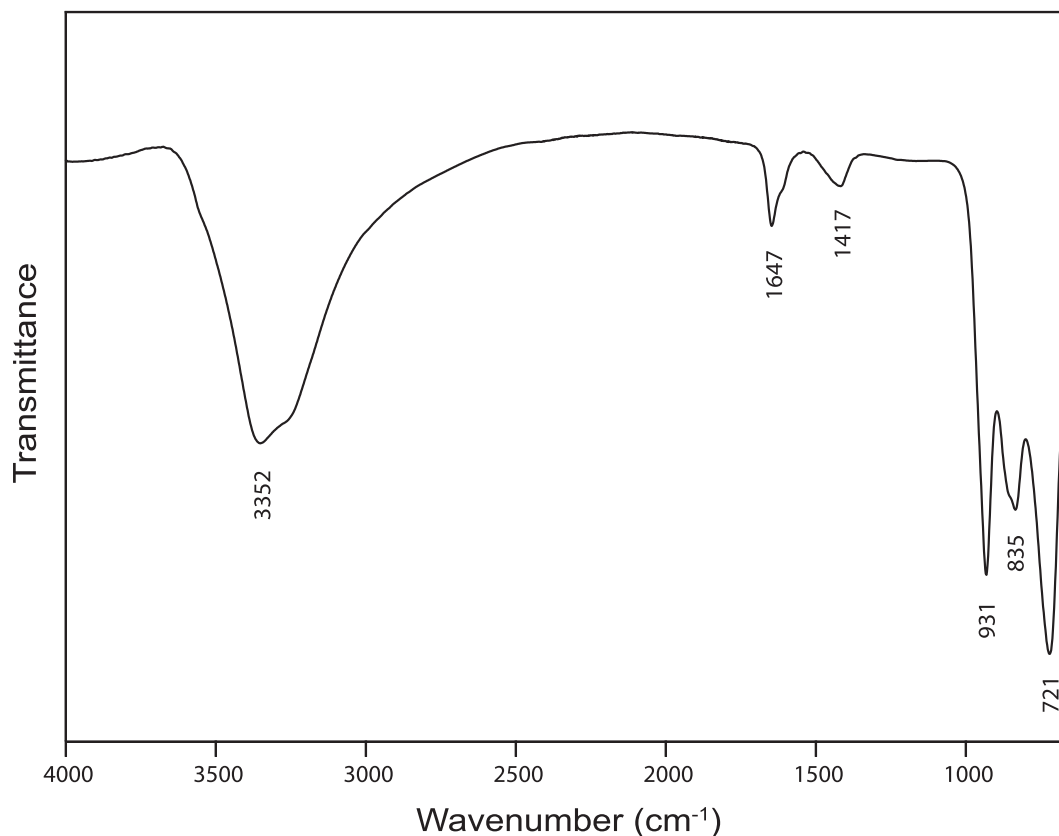


Fig. 4. Fourier-transform infrared spectrum of powdered kingsgateite.

Table 2. Powder X-ray diffraction data (d in Å) for kingsgateite.*

l_{obs}	d_{obs}	d_{calc}	l_{calc}	hkl	l_{obs}	d_{obs}	d_{calc}	l_{calc}	hkl
70	5.734	5.7313	71	2 0 0	12	1.962	1.9696	22	2 0 6
4	4.945	4.9702	4	1 1 2	25	1.911	1.9104	29	6 0 0
5	4.744	4.7474	5	2 1 1			1.8982	4	5 2 3
52	4.227	4.2370	63	2 0 2	12	1.875	1.8764	16	5 3 2
44	3.626	3.6248	53	3 1 0			1.8637	5	6 1 1
3	3.226	3.2463	3	2 1 3			1.8280	1	6 0 2
100	3.134	3.1409	100	3 1 2	18	1.810	1.8154	27	3 1 6
		3.0823	4	3 2 1	3	1.772	1.7723	4	5 4 1
11	2.867	2.8657	10	4 0 0	6	1.741	1.7416	11	6 2 2
10	2.744	2.7578	9	2 0 4			1.7189	2	6 1 3
5	2.706	2.7146	5	4 1 1			1.6964	2	2 1 7
19	2.606	2.6079	21	4 0 2	5	1.687	1.6925	10	4 0 6
		2.5337	2	3 2 3			1.6671	5	5 3 4
17	2.481	2.4826	17	3 3 2	8	1.651	1.6567	15	3 3 6
9	2.369	2.3759	11	3 1 4			1.6465	3	5 4 3
3	2.312	2.3173	2	4 1 3	14	1.631	1.6329	24	6 0 4
4	2.251	{ 2.2554	3	4 3 1			1.6252	2	5 2 5
		2.2480	1	5 1 0	2	1.591	1.5896	4	6 4 0
9	2.113	{ 2.1185	9	4 0 4			1.5730	6	0 0 8
		2.0987	4	5 2 1			1.5704	12	6 2 4
4	2.018	{ 2.0305	6	1 1 6	7	1.567	{ 1.5649	1	3 2 7
		2.0117	1	4 3 3			1.5623	3	7 2 1

*The strongest lines are given in bold

confirmed by infrared spectroscopy (see below). The empirical formula based on 11 anions per formula unit is

$\text{Zr}_{0.88}\text{U}_{0.02}\text{Th}_{0.01}\text{Fe}_{0.04}\text{Mo}_{1.94}\text{S}_{0.07}\text{P}_{0.02}\text{O}_{6.90}\text{Cl}_{0.02}\text{OH}_{2.08}\cdot 2.00\text{H}_2\text{O}$.
The ideal formula is $\text{ZrMo}_2^+\text{O}_7(\text{OH})_2\cdot 2\text{H}_2\text{O}$ which requires ZrO_2 26.49, MoO_3 61.89, H_2O 11.62, Total 100 wt.%.

Table 3. Crystal data, data collection and refinement details.

Crystal data	
Space group	$I4_1cd$
a, c (Å)	11.4626(16), 12.584(3)
V (Å ³), Z	1653.4(6), 8
$F(000)$	1696.0
μ (mm ⁻¹)	4.27
Absorption correction	multi-scan, $T_{\text{min}}, T_{\text{max}} = 0.39, 0.43$
Crystal dimensions (μm)	35 × 30 × 5
Data collection	
Temperature (K)	100
Radiation	Synchrotron, $\lambda = 0.710754$ Å
Crystal detector distance (mm)	108.031
θ range (°)	3.555–29.571
h, k, l ranges	–15 → 15, –15 → 15, –17 → 17
Total reflections measured	13501
Unique reflections	1159 ($R_{\text{int}} = 0.0404$)
Refinement	
Refinement on	F^2
R_1^* for $F_0 > 4\sigma(F_0)$.	4.53%
wR_2^\dagger for all F_0^2	10.67%
Reflections used $F_0^2 > 4\sigma(F_0^2)$	1159
Number of parameters refined	68
Goof	1.103
$\Delta/\sigma_{\text{max}}$	0.000
$\Delta\rho_{\text{max}}, \Delta\rho_{\text{min}}$ (e ⁻ /Å)	5.495, –2.132

* $R_1 = \sum ||F_o| - |F_c|| / \sum |F_o|$

$^\dagger wR_2 = \{ \sum [w(F_o^2 - F_c^2)^2] / \sum [w(F_o^2)^2] \}^{1/2}$. $w = 1 / [\sigma^2(F_o^2) + (aP)^2 + bP]$ where a is 0. 0.0911, b is 0. 4.20 and P is $[2F_c^2 + \text{Max}(F_o^2, 0)] / 3$

Infrared spectroscopy

An infrared-absorption spectrum of powdered kingsgateite (Fig. 4) was recorded using a Nicolet 5700 FTIR spectrometer

Table 4. Fractional atomic coordinates and displacement parameters (in Å²) for kingsgateite.

Atom	x	y	z	U_{eq}	U^{11}	U^{22}	U^{33}	U^{12}	U^{13}	U^{23}
Zr	0.5	0.5	0.28159(16)	0.0108(3)	0.0086(4)	0.0081(4)	0.0155(6)	0	0	0.0007(2)
Mo	0.66375(5)	0.52379(6)	0.54984(9)	0.0124(3)	0.0070(4)	0.0133(4)	0.0168(4)	0.0003(4)	0.0005(2)	-0.00018(16)
O1	0.6608(13)	0.6749(7)	0.5534(9)	0.020(2)	0.012(4)	0.009(3)	0.039(5)	0.003(4)	-0.001(3)	-0.005(2)
O2	0.6141(5)	0.4954(5)	0.4185(5)	0.0183(15)	0.012(3)	0.026(3)	0.017(2)	-0.0045(19)	-0.0016(19)	-0.001(2)
O3	0.8194(6)	0.4944(8)	0.5399(9)	0.0190(16)	0.015(2)	0.018(3)	0.023(4)	0.002(3)	-0.001(3)	0.001(3)
O4	0.5	0.5	0.6094(12)	0.013(3)	0.005(3)	0.020(5)	0.014(7)	0	0	0.000(3)
OH5	0.6786(5)	0.5072(7)	0.7176(8)	0.0182(17)	0.010(3)	0.020(3)	0.025(5)	-0.001(3)	0.000(3)	-0.0027(19)
OW6	0.6590(12)	0.3249(7)	0.5740(9)	0.022(2)	0.019(4)	0.007(3)	0.039(5)	-0.003(3)	-0.005(5)	0.002(2)

Table 5. Selected interatomic distances (Å) for kingsgateite.

Zr–O3 ×2	2.074(7)	Mo–O1	1.733(8)
Zr–O2 ×2	2.164(6)	Mo–O2	1.778(7)
Zr–O4	2.167(14)	Mo–O3	1.820(7)
Zr–OH5 ×2	2.202(7)	Mo–O4	2.040(5)
<Zr–O>	2.150	Mo–OH5	2.127(10)
		Mo–OW6	2.301(9)
		<Mo–O>	1.967

Table 6. Bond-valence analysis for kingsgateite.

	Zr	Mo	Sum
O1		1.63	1.63
O2	0.54 × ² ↓	1.43	1.97
O3	0.67 × ² ↓	1.27	1.94
O4	0.54	0.68 × ² →	1.90
OH5	0.49 × ² ↓	0.53	1.02
OW6		0.32	0.32
Sum	3.94	5.86	

Bond valence parameters are from Gagné and Hawthorne (2015).

equipped with a Nicolet Continuum IR microscope and a diamond-anvil cell. The spectrum shows a strong broad band centred on 3352 cm⁻¹ and with a shoulder at 3266 cm⁻¹ that is assigned to ν(OH) stretching vibrations. A medium strong band at 1647 cm⁻¹ with a shoulder at 1614 cm⁻¹ is attributed to the ν₂(δ)(H₂O) bending vibration and a band at 1417 cm⁻¹ may be due to Zr–OH bending vibrations (eg. Sarkar *et al.*, 2007). Bands at 931 cm⁻¹, 835 cm⁻¹ and 721 cm⁻¹ are attributed to ν (Mo–O) stretching vibrations.

Powder X-ray diffraction

Powder X-ray diffraction data (Table 2) for kingsgateite were recorded using a Rigaku R-Axis Rapid II curved imaging plate microdiffractometer with monochromatised MoKα radiation. A Gandolfi-like motion on the φ and ω axes was used to randomise the sample. Observed *d* values and intensities were derived by profile fitting using JADE 2010 software (Materials Data, Inc.). Unit-cell parameters refined from the powder data using JADE 2010 with whole pattern fitting are as follows: *a* = 11.489(4), *c* = 12.538(4) Å and *V* = 1655.0(13) Å³.

Crystal structure

A crystal fragment was attached to a MiTeGen polymer loop and single-crystal X-ray diffraction data were collected at the MX2 beamline of the Australian Synchrotron (Aragao *et al.*, 2018).

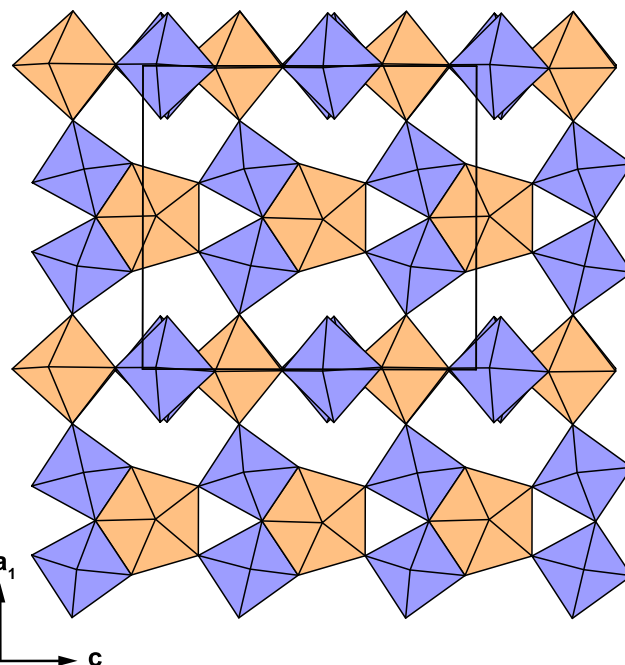


Fig. 5. The crystal structure of kingsgateite viewed along the *a*₂ axis. Zr[O₂(OH)₂] polyhedra are orange; Mo[O₄(OH)(H₂O)] octahedra are blue. The unit cell is outlined.

Data were collected using a Dectris EigerX 16M detector and monochromatic radiation with a wavelength of 0.71075 Å. The intensity data sets were processed using XDS (Kabsch, 2010) without scaling and with absorption correction and scaling using SADABS (Bruker, 2001).

A structure solution was obtained in space group *I*4₁*cd* using SHELXT (Sheldrick, 2015a) within the WinGX program suite (Farrugia, 2012). This structure is consistent with the structural model for ZrMo₂O₇(OH)₂(H₂O)₂ reported by Clearfield and Blessing (1972). The structure was refined using SHELXL-2018 (Sheldrick, 2015b) to *R*₁ = 0.0453 on the basis of 1159 unique reflections *F*_o > 4σ(*F*_o). H atoms could not be located in difference-Fourier maps. Details of the data collection and the structure refinement are provided in Table 3, refined atom coordinates and anisotropic-displacement parameters are listed in Table 4, selected interatomic distances are given in Table 5, and bond-valence values, calculated using the parameters of Gagné and Hawthorne (2015), are given in Table 6. The crystallographic information files have been deposited with the Principal Editor of *Mineralogical Magazine* and are available as Supplementary material (see below).

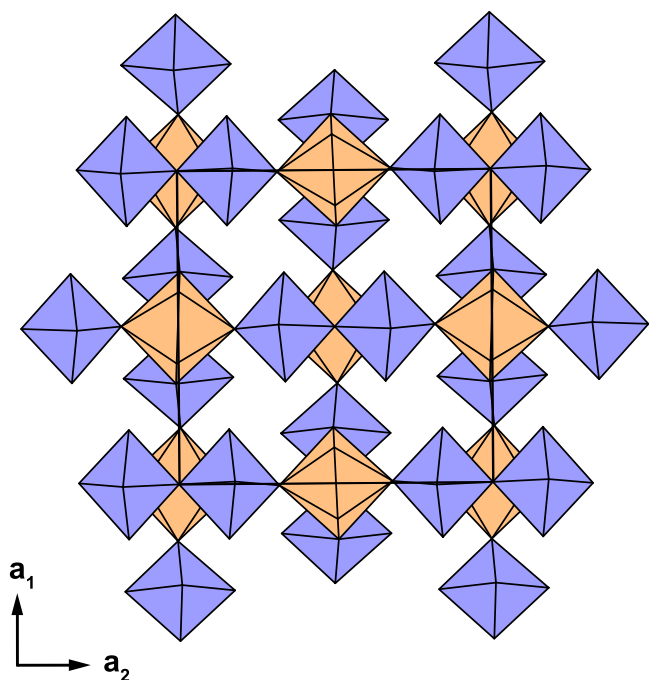


Fig. 6. The crystal structure of kingsgateite viewed along the c axis. Legend as in Fig. 5.

In the crystal structure of kingsgateite, there are two cation sites. The Zr site is [7]-coordinated by four O^{2-} atoms and two OH groups forming squat pentagonal bipyramids and with $\langle Zr-O \rangle = 2.150 \text{ \AA}$. The most common coordination number for Zr in mineral structures is [6]. Seven-coordinated Zr sites (pentagonal bipyramids) are found in the structures of several minerals, including baddeleyite, calzirtite, laachite, stefanweissite, voggite and zirconolite. The Mo site is [6]-coordinated by four O^{2-} atoms, one OH group and one H_2O group forming a distorted octahedron. The coordination is characterised by a short and a long apical bond distance (1.733 and 2.301 \AA) and equatorial bond distances that range from 1.778 to 2.127 \AA . This coordination geometry for Mo^{6+} cations has been observed in the structures of many in natural and synthetic molybdates, including the Bi molybdates gelsaite, koechlinite, sardignaite and mambertiite.

$Zr[O_5(OH)_2]$ polyhedra share equatorial edges with two Mo $[O_4(OH)(H_2O)]$ octahedra to form a $ZrMo[O_{11}(OH)_2](H_2O)_2$ cluster (Fig. 5). Clusters link by corner-sharing via O2 anions to form chains in the c direction. Chains are linked into a framework by corner-sharing via O3 anions along a_1 and a_2 (Fig. 6).

Although H atoms could not be located, four possible hydrogen bonds were identified based on $O \cdots O$ distances: $OH5 \cdots O1$ (2.774 \AA), $OH5 \cdots OW6$ (2.761 \AA), $OW6 \cdots O1$ (2.700 \AA) and $OW6 \cdots OH5$ (2.761 \AA). The observed $O_D \cdots O_A$ distances are consistent with H-bond valences of 0.19. Adding these respective H bond valence contributions results in satisfactory bond-valence sums at the anions.

Structural relations

Among minerals, kingsgateite is unique in terms of structure and chemistry. As noted, its synthetic analogue $ZrMo_2O_7(OH)_2 \cdot 2H_2O$, has been reported by Clearfield and Blessing (1972). The compound is a representative of a large group of synthetic compounds,

including Zr molybdates and tungstates, that have been studied for their promising cation-exchange properties. Most are amorphous, non-stoichiometric and non-equilibrium salts.

Zirconium tungstates in a crystalline form that are isostructural with $ZrMo_2O_7(OH)_2 \cdot 2H_2O$ have also been described. Clearfield and Blessing (1974) prepared Zr tungstate which was shown by powder X-ray diffraction to be isomorphous with $ZrW_2O_7(OH)_2 \cdot 2H_2O$. $ZrW_2O_7(OH,Cl)_2 \cdot 2H_2O$ was synthesised by Dadachov and Lambrecht (1997) and $ZrW_2O_7(OH_{0.984}Cl_{0.016})_2 \cdot 2H_2O$ by Cao *et al.*, (2006). The structures were refined using Rietveld refinement. The coordination (bond distances and angles) of the Zr and (Mo,W) sites in kingsgateite and in these compounds are not significantly different.

Supplementary material. To view supplementary material for this article, please visit <https://doi.org/10.1180/mgm.2022.43>

Acknowledgements. We thank Ben Wade of Adelaide Microscopy, The University of Adelaide for assistance with the microprobe analysis. The infrared spectrum was acquired with the assistance of the Forensic Science Centre, Adelaide. Structures Editor Peter Leverett and an anonymous reviewer are thanked for constructive comments that improved the quality of the manuscript. We thank John Haupt for providing the photograph of kingsgateite shown in Fig. 1. This research was undertaken in part using the MX2 beamline at the Australian Synchrotron, part of ANSTO, and made use of the Australian Cancer Research Foundation (ACRF) detector.

References

- Aragao D., Aishima J., Cherukuvada H., Clarken R., Clift M., Cowieson N.P., Ericsson D.J., Gee C.L., Macedo S., Mudie N., Panjikar S., Price J.R., Riboldi-Tunnicliffe A., Rostan R., Williamson R. and Caradoc-Davies T.T. (2018) MX2: a high-flux undulator microfocus beamline serving both the chemical and macromolecular crystallography communities at the Australian Synchrotron. *Journal of Synchrotron Radiation*, **25**, 885–891.
- Bruker (2001) SADABS. Bruker AXS Inc., Madison, Wisconsin, USA
- Cao Y.L., Deng X.B., Ma H., Wang S.F. and Zhao X.H. (2006) The synthesis and characterization of $ZrW_2O_7(OH_{1-x}Cl_x)_2 \cdot 2H_2O$ ($x = 0.016, 0.025$). *Defect and Diffusion Forum*, **251–252**, 21–26.
- Clearfield A. and Blessing R.H. (1972) The preparation and crystal structure of a basic zirconium molybdate and its relationship to ion exchange gels. *Journal of Inorganic and Nuclear Chemistry*, **34**, 2643–2663.
- Clearfield A. and Blessing R.H. (1974) The preparation of a crystalline basic zirconium tungstate. *Journal of Inorganic and Nuclear Chemistry*, **36**, 1174–1176.
- Clissold M.E., Leverett P., Sharpe J.L. and Williams P.A. (2008) Primary bismuth minerals from the Wolfram pipe, Kingsgate, New South Wales. *Australian Journal of Mineralogy*, **14**, 19–28.
- Dadachov M.S. and Lambrecht R.M. (1997) Synthesis and crystal structure of zirconium tungstate $ZrW_2O_7(OH,Cl)_2 \cdot 2H_2O$. *Journal of Materials Chemistry*, **7**, 1867–1870.
- Elliott P. and Kampf A.R. (2019) Kingsgateite, IMA 2019-048. CNMNC Newsletter No. 51. *Mineralogical Magazine*, **83**, 757–761, doi: 10.1180/mgm.2019.58
- England B.M. (1985) The Kingsgate mines, New South Wales, Australia. *The Mineralogical Record*, **16**, 265–289.
- Farrugia L.J. (2012) WinGX and ORTEP for Windows: an update. *Journal of Applied Crystallography*, **45**, 849–854.
- Gagné O.C. and Hawthorne F.C. (2015) Comprehensive derivation of bond-valence parameters for ion pairs involving oxygen. *Acta Crystallographica*, **B71**, 562–578.
- Kabsch W. (2010) XDS. *Acta Crystallographica*, **D66**, 125–132.
- Lawrence L.J. and Markham N.L. (1962) A contribution to the study of the molybdenite pipes of Kingsgate, NSW, with special reference to ore mineralogy. *Proceedings of the Australasian Institute of Mining and Metallurgy*, **203**, 67–94.

- Pouchou J.L. and Pichoir F. (1985) "PAP" $\sigma\rho Z$ procedure for improved quantitative microanalysis. Pp. 104–106 in: *Microbeam Analysis* (J.T. Armstrong, editor). San Francisco Press, California, USA.
- Sarkar D., Mohapatra D., Ray S., Bhattacharyya S., Adak S. and Mitra N. (2007) Synthesis and Characterization of Sol–Gel derived ZrO_2 doped Al_2O_3 nanopowder. *Ceramics International*, **33**, 1275–1282.
- Sharpe J.L. and Williams P.A. (2004) Secondary bismuth and molybdenum minerals from Kingsgate, New England district of New South Wales. *Australian Journal of Mineralogy*, **10**, 7–12.
- Sheldrick G.M. (2015a) SHELXT - Integrated space-group and crystal-structure determination. *Acta Crystallographica*, **A71**, 3–8.
- Sheldrick G.M. (2015b) Crystal structure refinement with SHELX. *Acta Crystallographica*, **C71**, 3–8.